A new green synthesis method of $CuInS_2$ and $CuInSe_2$ nanoparticles and their integration into thin films

Bensebaa, F.; Durand, C.; Aouadou, A.; Scoles, L.; Du, X.; Wang, D.; Le Page, Y.

Publisher's version / Version de l'éditeur:
https://doi.org/10.1007/s11051-009-9752-5
Journal of Nanoparticle Research, 12, 5, pp. 1897-1903, 2009

J Nanopart Res
DOI 10.1007/s11051-009-9752-5

RESEARCH PAPER

A new green synthesis method of $CuInS_2$ and $CuInSe_2$ nanoparticles and their integration into thin films

F. Bensebaa · C. Durand · A. Aouadou · L. Scoles · X. Du · D. Wang · Y. Le Page

Received: 2 April 2009 / Accepted: 31 August 2009

Abstract A new preparation method for $CuInS_2$ and $CuInSe_2$ nanoparticles synthesis is described without using any organic solvent. Heating Cu, In, and S/Se precursors dissolved in water for 30 min in a microwave oven in the presence of mercapto-acetic acid leads to monodispersed chalcopyrite nanoparticles. No precipitation of these nanoparticles is observed after several months at room temperature. These new materials have been thoroughly characterized to confirm their compositions, sizes, and structure without any filtration. Transmission electron microscopy (TEM) confirmed particle sizes below 5 nm. Energy dispersive X-ray analysis (EDXA) confirmed the chemical composition of these samples. X-ray diffraction (XRD) showed a chalcopyrite-type structure with crystallite size of about 2 nm. No difference has been observed between batch and continuous synthesis processes. Cu_xInS_2 and Cu_xInSe_2 nanoparticles, with $x < 1$, have been also synthesized and identified. Simulation using a commercial software confirmed the difference between copper poor (Cu_xInS_2) and copper rich ($CuInS_2$) chalcopyrite structures. Conventional spray deposition techniques have been used to form relatively thin films on solid substrates.

Keywords Nanoparticle · Green synthesis · Chalcopyrite · $CuInS_2$ · $CuInSe_2$ · Thin film · Photovoltaic · Environment

Introduction

Green chemistry principles applied to nanoparticle synthesis is attracting a lot of interest (Dahl et al. 2007). For example elimination of toxic reagents and solvents, increasing the yield and reducing purification steps and the amount of organic solvent, will help reduce fabrication cost and mitigate environmental impact. Nanoparticle synthesis in aqueous media will reduce utilization of organic solvent and could be also beneficial to filtration (Sweeney et al. 2006), integration and utilization steps involving aqueous media.

Chalcopyrite-type semiconductors have received a lot of interest in recent years for their potential use as photovoltaic materials for thin film-based solar cells (Dhere 2006; Kazmerski 2006). These chalcopyrite materials are called CIGS and usually correspond to the general formula $Cu(In_yGa_{1-y})S_zSe_{2-z}$ (where y and z vary from 0 to 1 and 0 to 2, respectively). Among inorganic photovoltaic materials, they display the highest optical absorption in the solar spectrum

F. Bensebaa (✉) · C. Durand · A. Aouadou · L. Scoles · X. Du · D. Wang · Y. Le Page
Institute for Chemical Process and Environmental Technology, National Research Council, 1200 Montreal Rd, Ottawa, ON K1A 0R6, Canada
e-mail: Farid.Bensebaa@nrc-cnrc.gc.ca

Published online: 29 September 2009

region. CIGS-based solar cells have been shown to provide the highest power efficiency among thin film cells, approaching those of crystalline silicon-based solar cells. Efficiency approaching 20% has been measured on a CIGS-based solar cell composition with an energy gap around 1.13 eV (Repins et al. 2008). However, the laborious process used to obtain these highly efficient CIGS solar cells is costly and requires precise multi-element co-evaporation under high vacuum and high temperature conditions. Furthermore, required post-deposition treatments often involve toxic gases such as H_2Se.

Low temperature and non-vacuum thin film deposition techniques using chalcopyrite nanoparticles and microparticles as starting material have been recently reported (Basol 2000; Eberspacher et al. 2001; Raffaelle et al. 2002; Kaelin et al. 2003, 2005; Kapur et al. 2003; Arici et al. 2004). Several prototypes have been described, but none of these approaches seems to have been successfully integrated into commercial photovoltaic solar cells. Physico-chemical parameters of these CIGS particles are often insufficiently characterized to allow optimized and reproducible properties of the photovoltaic solar cells. Furthermore, these particles are often too large to allow preparation of smooth, dense, and uniform films. For example, large particles may promote high porosity in films leading in turn to poor photovoltaic properties.

It is well known that nanoparticles melt at lower temperature than corresponding bulk material (Takagi 1954). However, significant reduction in melting temperature is observed on sub-10 nm nanoparticles only. This property allows a lower thermal energy budget during annealing of nanoparticle-based films. It is worth noting that annealing is a critical process in the fabrication of high quality films even when vacuum deposition techniques are used.

Various synthesis approaches have been recently developed specifically to produce sub-micron CIGS particles (Gurin 1998; Azad-Malik et al. 1999; Czekelius et al. 1999; Grisaru et al. 2003; Castro et al. 2004; Chun et al. 2005; Roh et al. 2005; Wei and Mu 2005; Dutta and Sharma 2006; Nakamura et al. 2006). There are very few cases where monodispersed chalcopyrite nanoparticles with a diameter around 5 nm or less are obtained. These targeted values for the particle size correspond to the estimated Bohr radius for $CuInSe_2$ and $CuInS_2$ semiconductor materials. A procedure to prepare nanoparticles with sub-5 nm diameter is critical to obtain high quality chalcopyrite films at low melting temperature.

$CuInS_2$ nanoparticles are obtained using polyvinylalcohol (Gurin 1998). Based on the diffraction peak width, an average crystallite size of 7 nm could be inferred. However, average diameter of the nanoparticle measured using TEM is relatively larger. Use of toxic gases (H_2S and H_2Se) and the presence of a difficult-to-remove polymer coating should be avoided when large scale production is sought. Using the so called TOPO approach, O'Brien's group showed that nanoparticles of $CuInSe_2$ are obtained with a diameter size in the range of 4–5 nm (Azad-Malik et al. 1999). A band edge of 420 nm (2.95 eV) is also measured. This band edge is outside the optimum solar absorption range. Using single source precursors, Castro et al. (2004) prepared colloidal $CuInS_2$ nanoparticles between 2.7 and 4 nm. The corresponding fabrication process involves several solvent and energy intensive size-selection steps, very costly to scale up.

Photovoltaic solar cells based on bulk $CuInS_2$ and $CuInSe_2$ (also referred to as CIS in the absence of Ga), respectively, with energy bandgap values of 1.5 and 1.0 eV have been shown to provide relatively high power efficiency (Klaer et al. 2003; Klenk et al. 2005; Shay et al. 1975). The structure and fabrication process of these two ternary compounds are relatively simple, providing a desirable combination of low cost and high efficiency for thin film solar cells. This is particularly true when compared to their quaternary and pentanary homologs (Dhere 2006; Kazmerski 2006; Repins et al. 2008). Calculation based on the solar spectrum distribution indicates that the highest efficiency solar cells are obtained with PV material having a bandgap between 1.2 and 1.8 eV, more specifically around 1.5 eV. However, the best efficiency obtained so far has been with chalcopyrite films with an energy bandgap around 1.13 eV (Repins et al. 2008).

Additional requirements related to fabrication cost and environmental footprint must be taken into account for any new material synthesis and process in view of a successful commercial applications. Specifically, the synthesis should be scalable, cost effective and involve "green" chemistry principles. Film deposition steps should avoid the need of energy

intensive processes. All processing should involve minimal heating without any toxic gases.

In this article, we will describe a microwave synthesis procedure to prepare $CuInS_2$ and $CuInSe_2$ nanoparticles. A microwave heating approach is used to prepare metallic and semiconductor nanoparticle (Grisaru et al. 2003; Bensebaa et al. 2005; Firth et al. 2005; Gardner et al. 2008). The choice of solvent to carry out nanoparticle synthesis is critical. Water is a well known solvent with a very high dielectric constant making it quite suitable for microwave heating. Proposed process should allow recycling of used water solvent. A water soluble surfactant should be used to avoid agglomeration and obtain size distribution with fairly uniform diameters. Ideally, the surfactant should be easily stripped away during the solar cell fabrication steps. These surfactants should then be weakly bonded to the nanoparticle. For this purpose, we have used Mercapto-acetic acid (MAA), although other surfactants may also work.

Experimental part

Cupric chloride dihydrate (Merck), indium chloride (Aldrich), and sodium sulphide (Aldrich) are the three precursors used to synthesize $CuInS_2$. Deionized water was used as solvent. MAA is used as surfactant. Copper and indium precursors are first mixed thoroughly with MAA to provide high dilution. Sodium sulphide (Na_2S) is then added to the previous solution. Cu:In:S atomic ratio of the starting materials is set to 1.1:1:2 to synthesize $CuInS_2$ nanoparticles. Atomic/molecular ratio of In:MAA is set to about 1:50.

The solution is then introduced inside the microwave and heated to about 90°C for 30 min using controlled ramping for a total duration of 2 min. Resulting solution is allowed to cool down. Centrifugation is also used to clean product reaction. After this cleaning step, solid material is used for characterization.

$CuInSe_2$ nanoparticles have been also prepared using the same approach. For the selenium source, Na_2Se precursor is used instead of Na_2S. Cu_xInS_2 and Cu_xInSe_2, with a nominal value of $x < 1$, have been prepared.

A dilute aqueous solution containing a few drops of the precipitate was prepared in a beaker and shaken vigorously. A drop of the resulting suspension was then deposited on a nickel grid and allowed to dry. Transmission electron microscopy (TEM) analysis was recorded using a Philips CM20 200 kV electron microscope equipped with an Oxford Instrument for Energy Dispersive X-ray Analysis (EDXA).

XRD characterization was performed at room temperature with Cu $K\alpha$ radiation using a Bruker diffractometer D8. CIGS powders were uniformly spread over a low background silicon based sample holder.

Result and discussion

We will first describe and discuss experimental data related to nanoparticle synthesis. Experimental data related to scalability of the nanoparticle synthesis and thin film integration will be then briefly discussed.

Nanoparticles synthesis

Colloidal $CuInS_2$ and $CuInSe_2$ nanoparticles obtained following microwave heating and cleaning steps are characterized to provide information about size distribution, composition, and structure. Following the microwave heating stage, colloidal nanoparticles are stable for several months in water solution at room temperature. Following cleaning and drying steps, these nanoparticles are easily redispersed in water and other solvent selected solvents.

Figure 1 shows a TEM image of as-synthesized $CuInS_2$ nanoparticles, representative of the overall field of view. Ultrafine, spherical, and well dispersed particles with uniform size distribution are shown. An average particle size of 3 nm is measured.

Using the so called TOPO method developed for the synthesis of monodispersed CdX (X = S, Se, Te) nanoparticles, Azad-Malik et al. (1999) showed a TEM micrograph of a single $CuInSe_2$ nanoparticle with a diameter of 4.5 nm. These authors also showed a relatively larger field of view TEM data of CuSe nanoparticles having an average size of about 15 nm.

Heating a single-source precursor $(PPh3)_2CuIn(SEt)_4$ up to 200°C or more in the presence of hexanethiol in dioctylphthalate leads to $CuInS_2$ nanoparticle with a diameter of 2–4 nm, following organic solvent based size-selection steps (Castro et al. 2004). TEM data showed some agglomeration.

Fig. 1 Transmission electron microscopy (TEM) image spectrum of as-synthesized $CuInS_2$ nanoparticles. Scale = 20 nm

However, it is worth noting that synthesis of this single source is quite difficult and laborious. Using similar precursors Gardner et al. synthesized clustered nanoparticle by microwave heating (Gardner et al. 2008).

Using a room temperature stirring for 5 h followed by 20 h aging and more as well as an elaborate post-treatment at 50 and 100°C, Wei and Mu (2005) obtained cube-shaped $CuInS_2$ nanoparticles with an average size of 27 nm.

$CuIn_yGa_{1-y}Se_2$ (or CIGS) nanoparticles with a diameter in the range of 30–80 nm were obtained using solvothermal technique. The temperature heating range of 180–280°C for around 36 h has been used min (Chun et al. 2005; Ahn et al. 2007). Irregular shaped particles with a wide size distribution have been obtained. CIGS nanoparticles with 15–70 nm diameter could be obtained by reacting under nitrogen atmosphere a mixture of CuI, InI_3, and GaI_3 in pyridine with Na_2Se in methanol at 0°C using mechanical stirring min (Chun et al. 2005; Ahn et al. 2007). The size of these nanoparticles are tunable from 15 to 70 nm when the reaction time is increased from 1 to 5 min (Chun et al. 2005; Ahn et al. 2007).

The two-step fabrication process used in this work to synthesize $CuInS_2$ nanoparticles gives rise to higher quality particles when compared to previously published data. We believe that combination of low temperature process and uniform heating process using microwave are key parameters allowing relatively high quality $CuInS_2$ nanoparticles. Furthermore, materials yield of this synthesis approach has been estimated to be above 90%. It is also worth noting that one could also consider the possibility of recycling the water used in the synthesis.

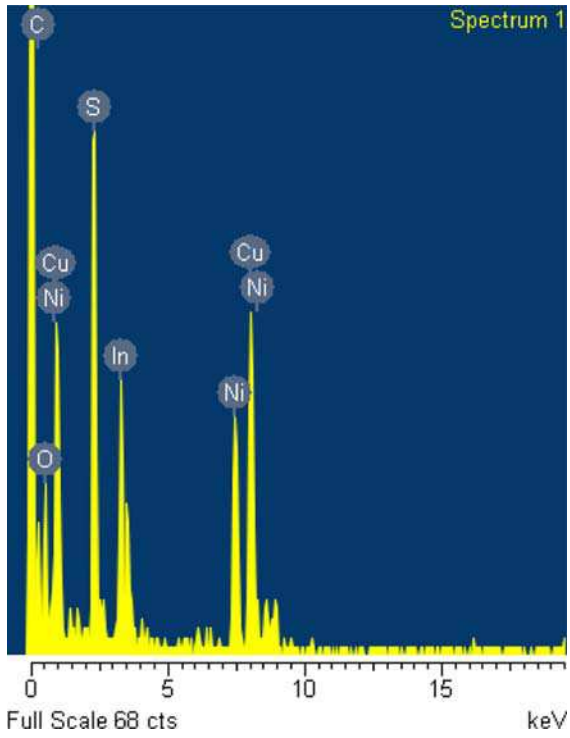

Fig. 2 Energy dispersive X-ray analysis (EDXA) of spectrum of as-synthesized $CuInS_2$ nanoparticle

EDXA data shown in Fig. 2 confirmed the chemical composition of the nanoparticle. Indeed, based on the peak intensity, an approximate relative ratio of Cu/In and Cu/S atomic ratio has been estimated. This ratio agrees with the nominal $CuInS_2$ stoichiometry. For precise determination of stoichiometry, one should use a reference sample, which we did not do in this study. Observed Ni peaks shown in Fig. 2 are assigned to the TEM sample holder.

X-ray diffraction (XRD) has been used to characterize the structure of these $CuInS_2$ nanoparticles. Figure 3 shows a typical diffraction pattern of this material. These patterns indicate that these nanoparticles have chalcopyrite tetragonal structure after comparing with the Joint Committee on Powder Diffraction Standards (JCPDS) card File No. 27-0159.

These diffraction patterns are similar to those reported in the literature (Czekelius et al. 1999). Three relatively broad diffraction peaks are detected around 2θ (2-theta) = 28°, 47°, and 55°. These three

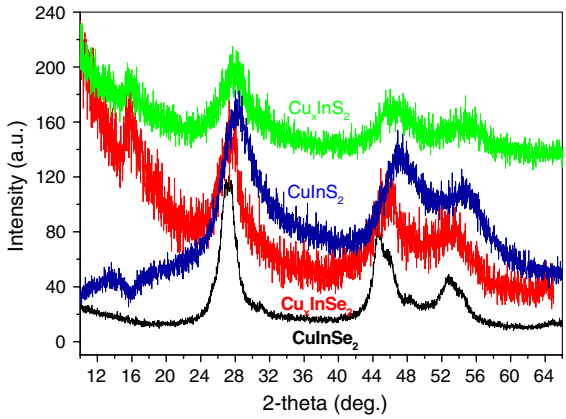

Fig. 3 X-ray diffraction (XRD) spectra of copper poor Cu_xInS_2 and Cu_xInSe_2 nanoparticles. XRD spectra of $CuInS_2$ and $CuInSe_2$ nanoparticles are also shown

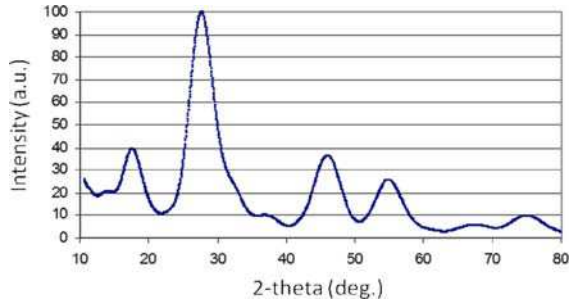

Fig. 4 Simulated X-ray diffraction (XRD) spectrum of Cu-poor $CuInS_2$ after averaging intensity data from nanoparticles with size of 2.0, 2.5, and 3.0 nm

peaks correspond to the (112), (204)/(220), and (116)/312 planes of the tetragonal structure, respectively (Czekelius et al. 1999; Akaki et al. 2003).

Line broadening of the XRD diffraction peaks has been used in the past to estimate the average crystallite size of analyzed particles. Peak broadening due to instrumental artefacts and strain are not considered here. The size of the crystallites d_c has been determined using the Scherrer equation (Castro et al. 2004; Gurin 1998; Nairn et al. 2006; Bensebaa et al. 2004)

$$d_c = 0.9\,\lambda/\beta\cos\theta$$

where β (in radians) is the linewidth at an angle 2θ (in radians) and λ is the X-ray wavelength, 1.5406 Å. Based on the linewidth of the (112) diffraction peak, we estimate the size of the crystallite to be around 2.2 nm. The small difference between the TEM (3 nm) and XRD (2 nm) dimensions could be explained by the presence of a dead layer at the surface of the crystallite. The relatively small size difference, around 0.8 nm, is a good indication of the mono-crystallinity of these nanoparticles.

$CuInSe_2$ nanoparticles have been also prepared after replacing Na_2S by Na_2Se as starting selenium raw material. The average particle size is slightly larger at around 4 nm. XRD peak feature of stoichiometric $CuInSe_2$ (Fig. 3) are consistent with those of $CuInS_2$ materials.

Ability to control the value of $x = [Cu]/[In]$ ratio in Cu_xInS_2 is highly desirable. Relative atomic concentrations of the starting raw materials have been varied to control the value of x in the final product. XRD peak features showed some differences between copper deficient (Cu_xInS_2) and stoichiometric ($CuInS_2$) nanoparticles. As shown in Fig. 3, a new peak is observed around $2\theta = 16°$ for Cu_xInS_2 and Cu_xInSe_2 (with $x < 1$) compositions.

XRD simulation with the exact Debye formula (Debye 1915) using a commercial software (Materials Toolkit) on small $CuInS_2$ nanoparticle confirmed that the relative intensity of this peak is related to copper deficiency (Le Page and Rodgers 2005). As shown in Fig. 4, decreasing Cu/In from 1 to 0.8, shows that the relative intensity of (110) peak at $2\theta = 16°$ increases. As expected XRD simulation of stoichiometric $CuInS_2$ do not show any significant peak from (110) plane.

Batch vs. continuous microwave synthesis process

Scalability of nanoparticle synthesis is also attracting interest in view of their potential industrial applications. Synthesis batch sizes are limited by the wavelength (around 12 cm) of the applied microwave (2.45 GHz). Using current commercial microwave systems, the size of the batch could be limited to double this critical microwave wavelength. A large number of batches will then be required to synthesize the kinds of amounts of these nanoparticles required for commercial-size applications. To optimize capital and human resources for the fabrication of nanoparticles, there is then some value in using a continuous synthesis process.

We have used two Fisher variable-flow peristaltic pumps for continuous supply and removal of precursors and reaction product, respectively. The first pump is used to introduce an appropriate volume of the aqueous solution, which containing the starting precursor mixtures into the reaction vessels. After 30 min of microwave reaction, the product is pumped out using the second pump. This process is repeated continuously. The product is centrifuged and analyzed with XRD. No difference has been observed between nanoparticles obtained with batch and continuous synthesis processes.

Thin film deposition of CIGS nanoparticles

Several coating techniques have been considered to deposit the CIGS nanoparticles on different substrates. In the past, precursor mixtures are deposited using doctor blading and screen printing techniques (Schulz et al. 1998; Eberspacher et al. 2001). These coating techniques are relatively easy to use and scale, although further processing steps are required. The main drawback of these techniques is the difficulty in obtaining thin film of about 2-μm thick or less. Spray deposition technique have been successfully used to deposit CIGS nanoparticle onto metal coated glass substrate (Schulz et al. 1998).

Air-brush spray deposition has been used to prepare high density film. First, about 5 μm TiO_2 film has been deposited on transparent conductive oxide (TCO) coated glass using doctor blading technique. TiO_2 slurry with an average size of 20 nm has been used. A concentrated solution of $CuInS_2$ nanoparticles has also been used for the spray deposition on top of the TiO_2 film. Following the deposition, the film was heated to about 400°C for 30 min. High density film $CuInS_2$ film has been obtained, confirmed by cross-section TEM data (Fig. 5). However, the quality of the film is not uniform across the whole surface. Indeed, small $CuInS_2$-free holes are observed. CIGS nanoparticles diffusion in the bulk of the TiO_2 film has been also observed by TEM. This observation is of interest toward the formation of an all inorganic 3D heterojunction at the interface between the CIGs materials and TiO_2 layer.

In light of the interest in fabricating thin film on flexible substrates, we have attempted to deposit these nanoparticles on titanium substrate. High density

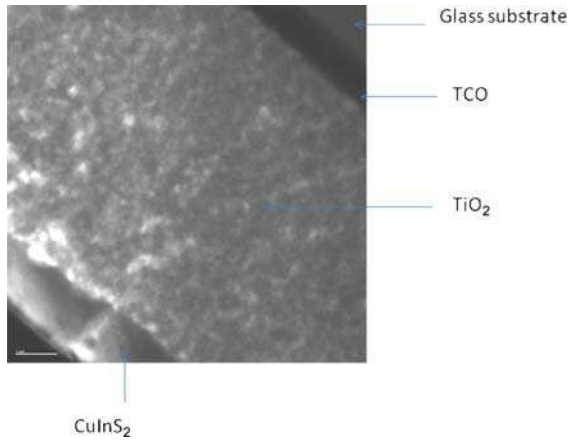

Fig. 5 TEM of $CuInS_2$ nanoparticle-based film obtained by spray deposition onto TiO_2 pre-coated TCO layer. Scale bar (*bottom left*) correspond to 1 μm

$CuInS_2$ film with a thickness around 1 μm has been obtained using spray deposition technique. XPS analysis of the Ti substrate, revealed the presence of about 10-nm thick TiO_2 layer. The thickness of this oxide layer could be tuned using different heat treatments. It is thus possible to perform monolithic integration of these nanoparticles directly on these potentially flexible TiO_2 coated Ti substrates.

Conclusion and perspective

We have synthesized high quality $CuInS_2$ and $CuInSe_2$ nanoparticles using a scalable process. Microwave heating for 30 min at around 90°C in water is used. Smooth thin films are obtained from these nanoparticles on different substrates, even at room temperature. Materials yield of this synthesis approach has been estimated to be above 90%. For the first time, Cu_xInS_2 and Cu_xInSe_2 nanoparticles, with $x < 1$, have been synthesized and identified unambiguously.

References

Ahn SJ, Kim KH, Chun YG, Yoon KH (2007) Nucleation and growth of Cu(In, Ga)Se_2 nanoparticles in low temperature colloidal process. Thin Solid Films 515:4036–4040

Akaki A, Komaki H, Yokoyama H, Yoshino K, Maeda K, Ikari T (2003) Structural and optical characterization of Sb-doped $CuInS_2$ thin films grown by vacuum evaporation method. J Phys Chem Solids 64:1863–1867

Arici E, Hope H, Schaffler F, Meissner D, Malik MA, Sariciftci NS (2004) Morphology effects in nanocrystalline CuInSe$_2$-conjugated polymer hybrid systems. Appl Phys A 79: 59–64

Azad-Malik M, O'Brien P, Revaprasadu N (1999) A novel route for the preparation of CuSe and CuInSe$_2$ nanoparticles. Adv Mater 11:1441–1444

Basol BM (2000) Low cost techniques for the preparation of Cu(In, Ga)(Se, S)$_2$ absorber layers. Thin Solid Films 361–362:514–519

Bensebaa F, Patrito N, Le Page Y, L'Ecuyer P, Wang D (2004) Tunable platinum–ruthenium nanoparticle properties using microwave synthesis. J Mater Chem 14:3378–3384

Bensebaa F, Farah A, Wang D, Bock C, Du X, Kung J, Le Page Y (2005) Microwave synthesis of polymer-embedded Pt–Ru catalyst for direct methanol fuel cell. J Phys Chem B 109:15339–15344

Castro SL, Bailey SG, Raffaelle RP, Banger KK, Hepp AF (2004) Synthesis and characterization of colloidal CuInS$_2$ nanoparticles from a molecular single-source precursor. J Phys Chem B 108:12429–12435

Chun YG, Kim KH, Yoon KH (2005) Synthesis of CuInGaSe$_2$ nanoparticles by solvothermal route. Thin Solid Film 480–481:46–49

Czekelius C, Hilgendorf M, Spanhel L, Bedja I, Lerch M, Muller G, Bloeck U, Su DS, Gersig M (1999) A simple colloidal route to nanocrystalline ZnO/CuInS$_2$ bilayers. Adv Mater 11:643–646

Dahl JA, Maddux BLS, Hutchison JE (2007) Toward greener nanosynthesis. Chem Rev 107:2228–2269

Debye P (1915) The scattering of X-rays. Ann Phys (Leipzig) 46:809–823

Dhere NG (2006) Present status and future prospects of CIGSS thin film solar cells. Sol Energy Mater Sol Cells 90:2181–2190

Dutta DP, Sharma G (2006) A facile route to the synthesis of CuInS$_2$ nanoparticles. Mater Lett 60:2395–2398

Eberspacher C, Frederic C, Pauls K, Serra J (2001) Thin-film CIS alloy PV materials fabricated using non-vacuum, particles-based techniques. Thin Solid Films 387:18–22

Firth AV, Tao Y, Wang D, Ding J, Bensebaa F (2005) Microwave assisted synthesis of CdSe nanocrystals for straightforward integration into composite photovoltaic devices. J Mater Chem 15:4367–4372

Gardner JS, Shurdha E, Wang C, Lau L, Rodriguez RG, Pak JJ (2008) Rapid synthesis and size control of CuInS$_2$ semiconductor nanoparticles using microwave irradiation. J Nanopart Res 10:633–641

Grisaru H, Palchik O, Gedanken A, Slifkin MA, Weiss AM, Palchik V (2003) Microwave-assisted polyol synthesis of CuInTe$_2$ and CuInSe$_2$ nanoparticles. Inorg Chem 42: 7148–7155

Gurin VS (1998) Nanoparticles of ternary semiconductors in colloids: low-temperature formation and quantum size effects. Colloids Sci 142:35–40

Kaelin M, Rudmann D, Kurdesau F, Meyer T, Zogg H, Tiwari AN (2003) CIS and CIGS layers from selenized nanoparticle precursors. Thin Solid Films 431–432:58–62

Kaelin M, Rudmann D, Kurdesau F, Meyer T, Zogg H, Tiwari AN (2005) Low-cost CIGS solar cells by paste coating and selenization. Thin Solid Films 480–481:486–490

Kapur VK, Bansal A, Le P, Asensio OL (2003) Non-vacuum processing of CuIn$_{1-x}$Ga$_x$Se$_2$ solar cells on rigid and flexible substrates using nanoparticle precursor inks. Thin Solid Films 431–432:53–57

Kazmerski LL (2006) Solar photovoltaics R&D at the tipping point: a 2005 technology overview. J Electron Spectrosc Relat Phenom 150:105–135

Klaer J, Luck I, Boden A, Klenk R, Gavilanes-Perez I, Scheer R (2003) Mini-modules from a CuInS$_2$ baseline process. Thin Solid Films 431–432:534–537

Klenk R, Klaer J, Scheer R, Lux-Steiner MC, Luck I, Meyer N, Ruhle U (2005) Solar cells based on CuInS$_2$—an overview. Thin Solid Films 480–481:509–514

Le Page Y, Rodgers JR (2005) Quantum software interfaced with crystal-structure databases: tools, results and perspectives. J Appl Cryst 38:697–705

Nairn JJ, Shapiro PJ, Twamley B, Pounds T, von Wandruszka R, Fletcher TR, Williams M, Wang C, Norton MG (2006) Preparation of ultrafine chalcopyrite nanoparticles via the photochemical decomposition of molecular single-source precursors. Nano Lett 6:1218–1223

Nakamura H, Kato W, Uehara M, Nose K, Omata T, Otsuka-Yao-Matsuo S, Miyazaki M, Maeda H (2006) Tunable photoluminescence wavelength of chalcopyrite CuInS$_2$-based semiconductor nanocrystals synthesized in a colloidal system. Chem Mater 18:3330–3335

Raffaelle RP, Castro SL, Hepp AF, Bailey SG (2002) Quantum dot solar cells. Prog Photovolt Res Appl 10:433–439

Repins I, Contreras MJ, Egaas B, DeHart C, Scharf J, Perkins CL, To B, Noufi R (2008) Accelerated publication 19.9%-efficient ZnO/CdS/CuInGaSe$_2$ solar cell with 81.2% fill factor. Prog Photovolt Res Appl 16:235–239

Roh SJ, Mane RS, Pathan HM, Joo OS, Han SH (2005) Rapid growth of nanocrystalline CuInS$_2$ thin films in alkaline medium at room temperature. Appl Surf Sci 252:1981–1987

Schulz DL, Curtis CJ, Flitton FA, Weisner H, Keane J, Matson RJ, Jones MJ, Parilla PA, Noufi R, Ginley DS (1998) Cu-In-Ga-Se nanoparticle colloids as spray deposition precursors for Cu(In, Ga)Se$_2$ solar cell materials. J Electron Mater 27: 433–437

Shay JL, Wagner S, Kasper HM (1975) Efficient CuInSe$_2$/CdS solar cells. Appl Phys Lett 27:89–90

Sweeney SF, Woehrle GH, Hutchison JE (2006) Rapid purification and size separation of gold nanoparticles via diafiltration. J Am Chem Soc 128:3190–3197

Takagi M (1954) Electron diffraction study of liquid–solid transition of thin metal films. J Phys Soc Jpn 9:359–363

Wei Q, Mu X (2005) Synthesis of CuInS$_2$ nanocubes by a wet chemical process. J Dispers Sci Technol 26:555–558